Applied Catalysis B: Environmental 198 (2016) 254–265

Contents lists available at ScienceDirect

Applied Catalysis B: Environmental

journal homepage: www.elsevier.com/locate/apcatb

Enhancement of catalytic performance of Ni based mesoporous alumina by Co incorporation in conversion of biogas to synthesis gas

Huseyin Arbag [a], Sena Yasyerli [a], Nail Yasyerli [a], Gulsen Dogu [a,*], Timur Dogu [b]

[a] Department of Chemical Engineering, Gazi University, 06570 Ankara, Turkey
[b] Department of Chemical Engineering, Middle East Technical University, 06680 Ankara, Turkey

ARTICLE INFO

Article history:
Received 12 March 2016
Received in revised form 24 May 2016
Accepted 27 May 2016
Available online 28 May 2016

Keywords:
Mesoporous alumina
Sol-gel
Dry reforming of methane
Bimetallic catalyst
Nickel-cobalt

ABSTRACT

Mesoporous alumina with an ordered pore structure has significant advantages as a catalyst support in terms of minimization of diffusion limitations and coke formation during reforming reactions. Conversion of biogas to synthesis gas through dry reforming of methane, was investigated over Co & Ni impregnated mono- and bi-metallic mesoporous alumina catalysts with ordered pore structures. Comparison of the results obtained with mesoporous alumina catalysts containing 5% Ni and 2.5% Ni-2.5% Co proved that incorporation of cobalt caused significant improvement in activity, as well as stability of the catalyst. Coke formation was also significantly decreased as a result of Co incorporation. Cobalt was found to be in reduced (metallic) state in this active catalyst. However, cobalt could not be reduced up to 750 °C in the catalyst containing only 5% Co in mesoporous alumina. In fact, the activity of this catalyst was negligibly low for dry reforming of methane. In this case, strong interaction of cobalt with alumina resulted in the formation of cobalt aluminate, which was difficult to reduce. However, in the case of bi-metallic catalyst, an alloy of Ni—Co was formed and reducibility of this alloy was much better than the reducibility of both 5Co@SGA and 5Ni@SGA. In conclusion, it was shown that bi-metallic Ni—Co based mesoporous alumina supported catalytic material was highly promising for conversion of biogas to synthesis gas, giving stable H_2 and CO selectivity values with coke minimization.

1. Introduction

Dry reforming of methane is the first step of conversion of two of the most abundant greenhouse gases (CH_4 and CO_2) present in biogas to synthesis gas [1–3]. Synthesis gas produced as a result of this catalytic process can then be used as a resource in Fischer-Tropsch synthesis, methanol synthesis, dimethyl ether synthesis etc., for the production of valuable chemicals and non-petroleum fuels. According to the stoichiometry of dry reforming reaction, the ratio of H_2 to CO is expected to be one in the product stream.

$$CH_4 + CO_2 \leftrightarrow 2CO + 2H_2 \quad \Delta H^{\bullet}_{298} = 247\ kJ\ mol^{-1} \tag{R.1}$$

However, occurrence of reverse water gas shift reaction (RWGS) causes some decrease of H_2/CO ratio in the product stream.

$$CO_2 + H_2 \leftrightarrow CO + H_2O \quad \Delta H^{\bullet}_{298} = 41\ kJ\ mol^{-1} \tag{R.2}$$

Other side reactions, such as methanation reaction (R.3) and steam reforming of methane (R.4) may also take place together with dry reforming reaction and may affect the product distribution [4,5].

$$CO_2 + 4H_2 \leftrightarrow CH_4 + 2H_2O \quad \Delta H^{\bullet}_{298} = -165\ kJ\ mol^{-1} \tag{R.3}$$

$$CH_4 + H_2O \leftrightarrow CO + 3H_2 \quad \Delta H^{\bullet}_{298} = 206\ kJ\ mol^{-1} \tag{R.4}$$

An important problem faced during dry reforming of methane is coke formation through dissociation of methane (R.5) and/or Boudouard reaction (R.6). Occurrence of coke may cause catalyst deactivation and clogging of the reactor. Depending upon the catalyst type and composition, decomposition reaction of methane becomes significant at temperatures higher than 550–600 °C [6,7]. However, due to its exothermic nature, thermodynamics of Boudouard reaction is favored at low temperatures.

$$CH_4 \rightarrow C + 2H_2 \quad \Delta H^{\bullet}_{298} = 75\ kJ\ mol^{-1} \tag{R.5}$$

$$2CO \leftrightarrow C + CO_2 \quad \Delta H^{\bullet}_{298} = -173\ kJ\ mol^{-1} \tag{R.6}$$

Due to major drawbacks of coke formation, recent studies on dry reforming of methane were focused on development of new catalysts with high coking resistance and stable catalytic perfor-

* Corresponding author.
E-mail address: gdogu@gazi.edu.tr (G. Dogu).

http://dx.doi.org/10.1016/j.apcatb.2016.05.064
0926-3373/

mance [8–12]. Group VIII B metals, like Co, Ni, Pt, Ru, Rh etc., were reported to show high catalytic activity in dry reforming of methane [1,13–19]. Among these materials, Ni and Co based catalysts attracted major attention of researchers, due to their high activity and availability at lower cost [5,8,13,17,19–23]. Although Ni based catalysts were highly active in reforming reactions, catalyst instabilities due to coke formation was reported as the main problem [5,8–12]. Effects of different promoters, such as Ce, Mg, Ca, etc., on coke minimization were discussed in the recent literature [9,13,24–26]. As it was shown in our earlier publications, incorporation of small amount of Rh or Ru was also shown to improve catalytic performance and stability of Ni based catalysts in dry reforming of methane [25,27].

As for the catalytic performance of cobalt is considered, there are conflicting results published in the literature. In the work of San-Jose-Alonso et al., it was reported that Co impregnated commercial γ-alumina gave much higher activity than the bi-metallic Co—Ni impregnated alumina catalysts [17]. However, in number of other studies, which were performed with bi-metallic Ni—Co catalysts prepared following different routes and different supports, it was reported that synergic effect between Ni and Co caused much better catalytic performance than monometallic catalysts, in reforming reactions [8,22,28,29]. Type of support material used, differences of calcination/reduction temperatures and synthesis procedures of these catalysts were expected to have significant effects on their catalytic performances. Catalytically active state of cobalt is its metallic form. Oxidation of cobalt during reaction or presence of its higher oxidation states due to interaction with the catalyst support material are expected to decrease the activity of cobalt based catalysts in reforming reactions. In fact, in a recent publication of our research group for steam reforming of ethanol (SRE) over Co based alumina catalysts, it was reported that formation of cobalt aluminate phase caused significant reduction of the activity of this material [30]. However, in the case of using mesoporous magnesium aluminate as the support material of Co impregnated catalyst, cobalt was in metallic state and its activity was very high in SRE [30].

Effect of catalyst support material has also been shown to be quite important from the point of view of catalytic performance and coke formation [19,22,24,28–35]. Mesoporous catalyst supports with ordered pore structure were shown to cause less diffusion resistance of reactants to the active sites and less susceptible to catalyst deactivation due to pore blockage by coke deposition, than the conventional microporous materials [19,25,27–30,36]. Mesoporous alumina with an ordered pore structure (MA) is a highly stable catalyst support with high surface area and large pore diameters in the range of 6–10 nm [5,12,30]. As it was shown in our recent publications, coke minimization could also be achieved by incorporation of tungsten oxide into Ni based mesoporous alumina catalysts [5,12]. Interaction of the active metal with the support is strongly related to the nature of the support and also to the catalyst synthesis route. Such interactions are expected to have strong influence on the activity of reforming catalysts, as well as their stability and coke formation.

Synthesis of mesoporous alumina incorporated Ni—Co bi-metallic catalysts and investigation of the effects of interaction of these metals with the mesoporous alumina support in dry reforming of methane, are the main objectives of the present study. In the present study, Co & Ni impregnated mono- and bi-metallic mesoporous alumina catalysts with ordered pore structures were synthesized and their catalytic performances were compared in dry reforming of methane. Increase of catalytic performance and stability, as well as coke minimization was illustrated, as a result of modification of Ni impregnated mesoporous alumina by Co incorporation.

2. Experimental

2.1. Synthesis and characterization of the catalytic materials

A highly stable mesoporous alumina catalyst support material with ordered pore structure was synthesized following a sol-gel route (SGA). Details of the synthesis procedure of the mesoporous sol-gel alumina were reported in an earlier publication of ours [5]. In this procedure, aluminum isopropoxide was used as the alumina precursor. It was dissolved in hot deionized water at 85 °C, with continuous stirring. Nitric acid (HNO_3) was then added to start the hydrolysis reaction, resulting in a sol. Then, 1,3-butanediol was added, while stirring. The solution was kept on stirring for 24 h and then it was kept at 60 °C to form the gel. After formation of the gel, sample was dried at 100 °C for 24 h and then the solid product was calcined at 800 °C, for 6 h. In the preparation of Ni and/or Co incorporated catalysts, nickel nitrate hexahydrate ($Ni(NO_3)_2.6H_2O$) and cobalt nitrate hexahydrate ($Co(NO_3)_2.6H_2O$) were used as the Ni and Co sources, respectively. Mesoporous alumina supported bi-metallic catalyst, containing 2.5% Ni and 2.5% Co, and monometallic catalysts containing 5% Ni (5Ni@SGA) or 5% Co (5Co@SGA) were synthesized following wet impregnation routes. Mesoporous alumina support was dispersed in deionized water. Salts of Ni and Co were also separately dissolved in deionized water, at 40 °C. Solutions containing nickel and/or cobalt ions were then added to the catalyst support mixture, drop by drop. Evaporation of water was then achieved at 40 °C, while stirring. Dried material was calcined in a tubular furnace under the flow of dry air. Temperature of the furnace was increased at a heating rate of 1 °C/min, until 800 °C was reached. Calcination was then continued for 6 h at 800 °C. In the case of bi-metallic catalysts containing 2.5% Ni and 2.5% Co, simultaneous impregnation of Ni and Co was achieved, before the calcination and the reduction steps. This material was denoted as 2.5Co-2.5Ni@SGA. These catalytic materials were then reduced at 750 °C in a flow of hydrogen for three hours, before the reaction tests.

Nitrogen adsorption–desorption, X-ray diffraction (XRD), X-ray photoelectron spectroscopy (XPS), scanning electron microscopy combined with energy-dispersive X-ray spectroscopy (SEM-EDX), transmission electron microscopy (TEM-EDX mapping) and temperature programmed reduction (TPR) techniques were used for the characterization of the synthesized catalytic materials. XRD, N_2 adsorption–desorption, thermal analysis (TGA-DTA) and scanning electron microscopy (SEM) results of the spent catalysts gave information about coke deposition and structural stability of the catalytic materials. X-ray diffraction (XRD) patterns were obtained by a Rigaku Ultima-IV instrument with a Cu Kα radiation source (λ = 0.15406 nm). BET surface area values and the pore size distributions of the synthesized materials were measured by the nitrogen adsorption–desorption technique, using a Quanta Chrome-Autosorb-1C sorptometer. Scanning electron micrographs were also obtained by a QUANTA 400 F field emission instrument. TEM analysis was performed using a Jeol Jem-2100 F 200 kV HRTEM instrument. Temperature programmed reduction (TPR) curves of the synthesized materials were obtained using the Chembet 3000 instrument. Thermal analyses of the used catalysts were performed using a PerkinElmer Pyris instrument, in a flow of dry air.

2.2. Catalytic reactions

Dry reforming of methane was carried out in a flow reactor, consisting of a quartz tube with an inner diameter of 6 mm. A feed stream with a composition of $CH_4/CO_2/Ar = 1/1/1$ was fed to the reactor at a flow rate of 60 ml/min, measured at atmospheric conditions. Catalyst particles synthesized in this study were pelletized, crushed and sieved to 1–2 mm in size and 0.1 g of these

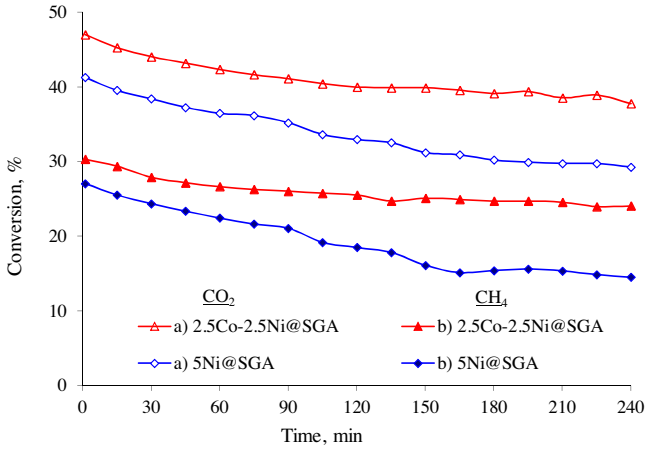

Fig. 1. Conversions of CO_2 and CH_4 over 5Ni@SGA and 2.5Co-2.5Ni@SGA catalysts reduced at 750 °C (Reaction conditions: 600 °C; 0.1 g catalysts; total flow rate of 60 ml/min with a $CH_4/CO_2/Ar = 1/1/1$ ratio).

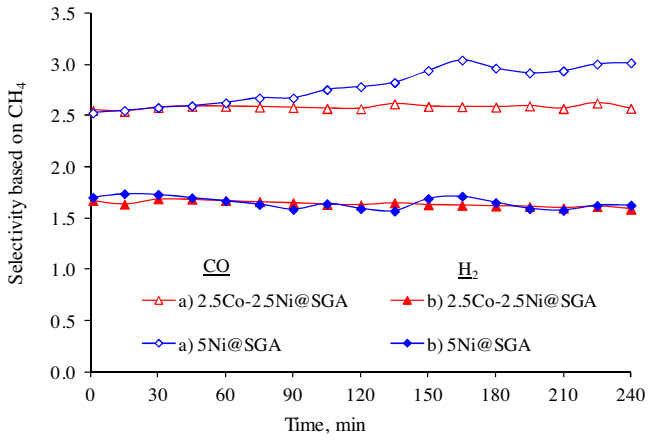

Fig. 2. Hydrogen and CO selectivity values with respect to converted methane over 5Ni@SGA and 2.5Co-2.5Ni@SGA catalysts reduced at 750 °C (Reaction conditions: 600 °C; 0.1 g catalysts; total flow rate of 60 ml/min with a $CH_4/CO_2/Ar = 1/1/1$ ratio).

particles was loaded to the reactor, by supporting from both ends with quartz wool. Experiments were performed at a space velocity of 36000 ml/(g_{cat} h). Activity tests were performed at 600 °C and 750 °C. Reaction products were analyzed by a gas chromatograph (PerkinElmer Autosystem XL GC) which was connected on-line to the reactor exit. This GC was equipped with a thermal conductivity detector (TCD) and a Carbosphere column. Catalytic performances of the synthesized materials were evaluated in terms of conversions of CO_2 and CH_4 (defined by Eqs. (1) and (2)), as well as H_2, CO selectivity values evaluated with respect to converted CH_4 (defined by Eqs. (3) and (4)).

$$CH_4\ \text{Conversion} = \frac{(CH_{4(in)} - CH_{4(out)})}{CH_{4(in)}} \times 100 \quad (1)$$

$$CO_2\ \text{Conversion} = \frac{(CO_{2(in)} - CO_{2(out)})}{CO_{2(in)}} \times 100 \quad (2)$$

$$H_2\ Selectivity = \frac{H_{2(out)}}{(CH_{4(in)} - CH_{4(out)})} \quad (3)$$

$$CO\ Selectivity = \frac{CO_{(out)}}{(CH_{4(in)} - CH_{4(out)})} \quad (4)$$

3. Results and discussions

3.1. Activity test results

Most of the dry reforming activity tests were performed at 600 °C at a space velocity of 36000 ml/(g_{cat}.h). Variation of methane and carbon dioxide conversion values obtained with the mesoporous alumina catalyst, containing only 5% Ni (5Ni@SGA), are shown in Fig. 1. These activity tests were performed within a reaction period of 240 min. According to the stoichiometry of dry reforming reaction (Eq. (1)), equal conversion values were expected for these two reactants. Higher conversion of CO_2 than the conversion of CH_4 was mainly due to contribution of RWGS reaction. Considering that the space time within the reactor was only about 0.1 s, activity of this catalyst was quite high, giving initial CH_4 and CO_2 conversion values of 28% and 41%, respectively. According to the thermodynamics of dry reforming and water gas shift reactions, equilibrium conversions of methane and carbon dioxide were expected as 46% and 58% respectively, at the reaction temperature of 600 °C.

Decrease of conversion values of both CH_4 and CO_2 with respect to reaction time, indicated catalyst deactivation, probably due to coke deposition (Fig. 1). Although the conversions of both CH_4 and CO_2 decreased as a function of reaction time, decrease of conversion of CH_4 was more significant than the decrease of conversion of CO_2. In fact, the ratio of conversion values of CO_2 and CH_4 increased from 1.46 to 2.14 within the reaction period of 240 min. As it was discussed before, occurrence of RWGS reaction is the main reason of having higher conversion values of CO_2 than the conversion values of CH_4. Hence, the increase of the ratio of the conversion values of CO_2 to CH_4 with reaction time could be due to the higher contribution of RWGS reaction to the product distribution than the dry reforming reaction, at longer reaction times. Apparently, deactivation rate of the RWGS reaction was less than the deactivation rate of dry reforming reaction. Product distributions shown in Fig. 2 supported this conclusion, giving an increase of CO/H_2 selectivity ratio from 1.6 to 2.0 within the same reaction period. CO and H_2 selectivity values reported in Fig. 2 were based on converted amount of CH_4. In the absence of RWGS reaction, selectivity values of both CO and H_2 would be expected as 2. However, due to the occurrence of RWGS reaction, an increase in CO selectivity and a decrease in H_2 selectivity were expected. Hence, increased contribution of RWGS reaction to the product distribution would cause an increase in this selectivity ratio. Clearly, coke deposition as a result of methane decomposition and/or Boudouard reaction might also have some contribution to the product distribution.

It was quite surprising to observe that 5Co@SGA catalyst showed almost no catalytic activity in dry reforming of methane. This result contrasted with the result reported by San-Jose-Alonso et al. [17], reporting that γ-alumina supported cobalt (9%) gave quite high activity in dry reforming. Main differences of the two studies were the nature of support material (γ-alumina versus mesoporous alumina), reaction temperature and calcination/reduction conditions of the synthesized materials. In our case, the catalyst was calcined at 800 °C and then reduced at 750 °C, while the catalyst prepared by San-Jose-Alonso et al., was not calcined and it was only reduced at 500 °C. Apparently, in our case, impregnated cobalt strongly interacted with the mesoporous alumina support during its calcination step at 800 °C. This interaction caused formation of cobalt aluminate, which was very difficult to be reduced. Very low activity of cobalt impregnated mesoporous alumina, which was calcined at a high temperature, was also reported in the recent publication of our group for steam reforming of ethanol [30]. That observation had also been explained by the formation of cobalt aluminate during the calcination step of the catalyst. Formation of cobalt aluminate phase was also shown by Sengupta et al. and Das et. al., for the Co impregnated alumina catalysts which were calcined at tempera-

Table 1
Physical & chemical properties of synthesized catalysts.

Catalysts	Metal Content, %	BET Surface Area, m^2/g	Average Pore Size, nm	Pore Volume, cm^3/g
SGA	–	185	11.2	0.50
5Ni@SGA	5 Ni	113	11.3	0.38
5Co@SGA	5 Co	127	11.3	0.41
2.5Co-2.5Ni@SGA	2.5 Ni & 2.5 Co	139	11.3	0.42

tures higher than 973 K [38,39]. Their conclusions were justified by the UV–vis analysis of the synthesized materials. All these results showed the importance of calcination/reduction temperature of Co impregnated alumina on the nature of the catalyst and hence on its catalytic performance. This point is further justified later in this manuscript, basing on the characterization results of the catalysts synthesized in the present study.

Although 5Co@SGA showed no activity in dry reforming of methane, catalytic performance of 2.5Co-2.5Ni@SGA was very good at the same temperature (600 °C). In fact, the performance of 2.5Co-2.5Ni@SGA was even better than the performance of 5Ni@SGA. Initial conversion values of CH_4 and CO_2 were about 30% and 47% over 2.5Co-2.5Ni@SGA. These conversion values were somewhat higher than the corresponding conversion values observed over 5Ni@SGA, which were 28% and 41%, respectively. More importantly, much higher stability of CO and H_2 selectivity values were observed over 2.5Co-2.5Ni@SGA than 5Ni@SGA (Fig. 2). Product distributions shown in Fig. 2 clearly indicated highly stable hydrogen and carbon monoxide selectivity values over 2.5Co-2.5Ni@SGA. Apparently, replacement of half of the Ni with Co significantly improved the catalytic performance of the synthesized material, while the alumina supported catalyst containing 5% Co showed no activity. Synergic effect between these two metals was also discussed by Luisetto et al. [22] and Zhang et al. [28], for the catalysts prepared using co-precipitation methods and with different support materials, like ceria and Al—Mg—O, respectively. Basing on the catalyst characterization results reported in the following section of this manuscript, it was concluded that, in the case of bi-metallic catalysts containing Ni and Co, an alloy of Ni—Co was formed and this hindered strong interaction of cobalt with the alumina support. Formation of such an alloy structure was also reported in the work of Takanabe et al., over a titania supported cobalt-nickel catalyst. It was concluded in that work that, addition of some Ni to Co impregnated titania caused significant increase in activity and selectivity of the catalyst, by suppressing the oxidation of cobalt [37]. Improvements in the reducibility of the Co impregnated catalyst as a result of Ni addition and formation of a homogeneous Ni—Co alloy was also reported by Zhang et al., and Sengupta et al. [28,39]. These results were further discussed in the following sections by the differences of chemical and structural characteristics of 5Co@SGA and 2.5Co-2.5Ni@SGA.

3.2. Characterization results of the synthesized catalytic materials

Some physical and chemical properties of the synthesized catalysts are given in Table 1. Surface area of pure mesoporous alumina (SGA) was 192 m^2/g. As a result of impregnation of Ni and/or Co, BET surface area values decreased, indicating closure of some of the pores by impregnated Ni and/or Co. Decrease of pore volume as a result of Ni incorporation also supported this conclusion (Table 1).

Nitrogen adsorption/desorption isotherms of all of the catalytic materials are Type IV (Fig. 3a), indicating formation of mesoporous alumina structures. Pore size distributions of these materials showed that diameters of most of the pores were between 5 and 20 nm (Fig. 3b). Average pore sizes of these materials were

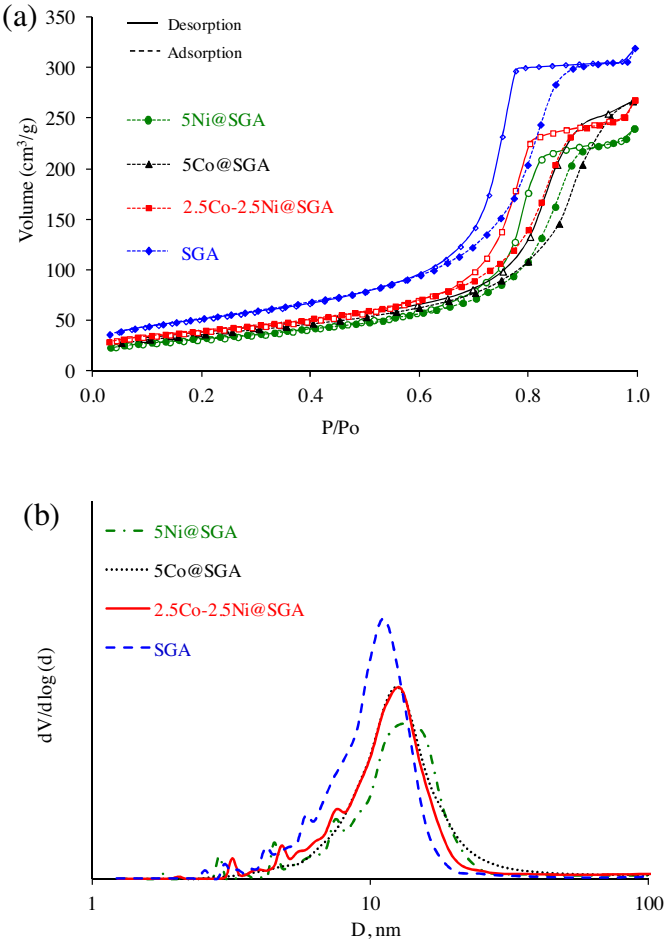

Fig. 3. N_2 adsorption-desorption isotherms (a) and pore size distributions (b) of mesoporous alumina (SGA), 5Ni@SGA, 5Co@SGA and bimetallic 2.5Co-2.5Ni@SGA catalysts, reduced at 750 °C.

about 11 nm. A decrease in pore volume indicated closure of some of the pores by incorporated nickel and/or cobalt.

SEM image and SEM-EDX mappings of Al, Co and Ni for 2.5Co-2.5Ni@SGA are shown in Fig. 4. Co and Ni mappings given in Fig. 4c & d clearly showed that both of these metals were very well dispersed within the mesoporous alumina support. TEM images indicated the presence of metal clusters of about 10 nm and well dispersion of Ni and Co within the mesoporous alumina support (Fig. 5).

In order to observe the reducibility of Co and Ni oxides within the synthesized catalytic materials, TPR analyses were performed with a H_2–N_2 stream containing 5% hydrogen. Reduction of pure NiO to Ni was expected to take place in the temperature range of 300–500 °C [40,41]. However, in the case of alumina supported NiO, increase of reduction temperature to the 550–900 °C range was reported, due to interaction of metal and the support material [40,42]. In the TPR analysis of Ni@SGA, a peak starting at about 700 °C was observed (Fig. 6a). Such a high reduction temperature indicated that nickel was in nickel aluminate spinel structure ($NiAl_2O_3$) in this material. Reduction temperature of $NiAl_2O_3$ was also reported in the literature as being in the temperature range of 700–800 °C [39,41]. Since the reduction temperature of the calcined catalytic materials was selected as 750 °C, reduction of most of Ni^{2+} to Ni^0 was expected within our catalysts. In the case of reduction of cobalt oxide, Co_3O_4 is expected to reduce to CoO and then to metallic Co within temperature ranges of 200–300 °C and 400–500 °C, respectively [43]. In our case, in the TPR analysis of 5Co@SGA, the peak observed in the temperature range of

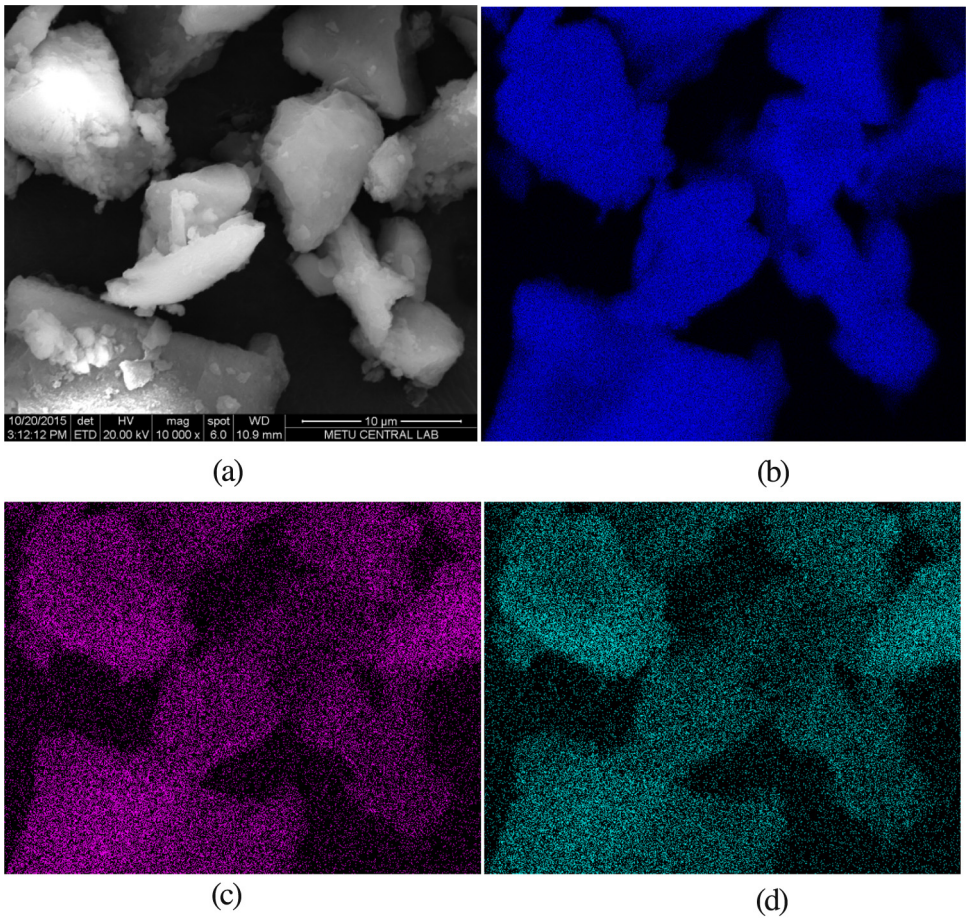

Fig. 4. SEM-EDX mapping of 2.5Co-2.5Ni@SGA fresh catalysts reduced at 750 °C: (a) image of sample; (b) Al mapping; (c) Co mapping; (d) Ni mapping.

200–300 °C was very small and there was no peak in the 400–500 °C range (Fig. 6b). This result indicated that the interaction of cobalt species with the mesoporous alumina support was very strong. This result implied that such a strong interaction resulted formation of cobalt aluminate during the calcination of 5Co@SGA, at 800 °C. Cobalt aluminate is highly stable and it is very difficult to reduce. In fact, in a recent publication of our research group for steam reforming of ethanol over Co based alumina catalysts, formation of cobalt aluminate phase and its inactivity in steam reforming of ethanol was also reported [30]. Formation of cobalt aluminate phase was also reported in the literature at calcination temperatures higher than 700 °C [37,38]. However, for the Co impregnated alumina catalysts which were calcined at lower temperatures, formation of cobalt aluminate was less probable. In fact, in the recent Fischer-Tropsch synthesis work of Shimura et al., cobalt impregnated alumina catalysts, which were calcined at 400 °C, gave two reduction peaks of cobalt oxide in the temperature ranges of 300–400 °C and 400–650 °C, in the TPR analysis [44]. These results clearly showed the importance of calcination/reduction temperatures of Co impregnated alumina catalysts on their catalytic performance. Inactivity of 5Co@SGA, which was synthesized in this study, was concluded to be due to the formation of $CoAl_2O_3$ phase, which could not be reduced at 750 °C. This result proved the importance of oxidation state of cobalt on its activity in dry reforming of methane. As it was also reported in the literature, the active form of cobalt was its metallic state for steam reforming and dehydrogenation reactions [45–47].These conclusions were further supported by the XPS and XRD analysis results of the catalytic materials synthesized in the present work.

In the case of 2.5Co-2.5Ni@SGA, TPR analysis showed a sharp reduction peak at the temperature range of 500–550 °C, with a shoulder extending up to 700 °C (Fig. 6c). This reduction peak observed in the TPR analysis of 2.5Co-2.5Ni@SGA showed that the reducibility of the bi-metallic catalyst was much better than the reducibility of Co and Ni impregnated catalysts, which were calcined at 800 °C. In the case of bi-metallic Ni—Co materials, an alloy of Ni—Co was expected to be formed [37,39]. Formation of such an alloy hindered the interaction of Ni and Co with the alumina support. Improvements in the reducibility of the Co impregnated catalyst as a result of Ni addition and formation of a homogeneous Ni—Co alloy was also reported in the literature [28,39]. XRD analysis of the synthesized materials, which were discussed later in this manuscript, also justified the formation of such an alloy. These results indicated that, cobalt oxide within this bi-metallic catalyst was in alloy form and could be reduced to Co^0 in a temperature range of 500–700 °C. Another peak was also observed in the TPR profile of 2.5Co-2.5Ni@SGA, at temperatures over 700 °C. This peak corresponds to the reduction of $NiAl_2O_3$ to metallic Ni. Better reducibility of cobalt in 2.5Co-2.5Ni@SGA was concluded to be the main reason of its better catalytic performance than the catalytic performance of 5Ni@SGA.

In order to have a better understanding of reduction process of bi-metallic catalytic materials, two other materials, containing 2.5% Co and 2.5% Ni, were also prepared following sequential impregnation procedures. In the first case, Ni was impregnated on SGA. After the calcination step of this material Co was impregnated over Ni containing SGA. This material was denoted as 2.5Co@2.5Ni@SGA. In the second case, first Co was impregnated. After the calcina-

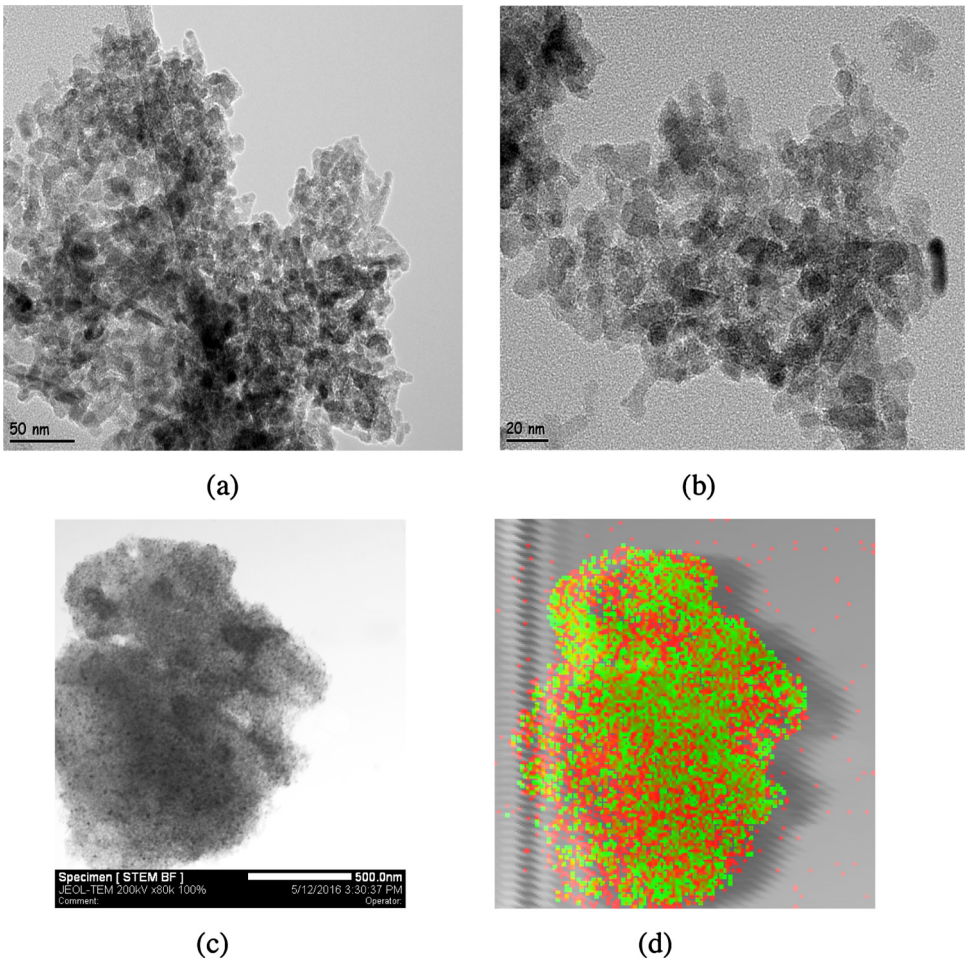

Fig. 5. (a & b)TEM images of 5Co@SGA; (c & d)TEM image and EDX mappings of 2.5Co-2.5Ni@SGA [Ni (green) Co (red)]. (For interpretation of the references to colour in this figure legend, the reader is referred to the web version of this article.)

tion step of this material, impregnation of Ni was performed. This material was denoted as 2.5Ni@2.5Co@SGA. TPR of the Co—Ni bimetallic catalysts which were synthesized following the sequential routes are shown in Figs. 6d and e, for 2.5Ni@2.5Co@SGA and 2.5Co@2.5Ni@SGA, respectively. Some important differences were observed in the TPR's of 2.5Co-2.5Ni@SGA and 2.5Co@2.5Ni@SGA and 2.5Ni@2.5Co@SGA. Sharp TPR peak observed in the temperature range of 500–600 °C for 2.5Co-2.5Ni@SGA was not observed in the TPR's of either 2.5Co@2.5Ni@SGA. In the case of 2.5Ni@2.5Co@SGA (Fig. 4d), a single reduction peak was observed in the temperature range of 700–780 °C range, corresponding to the reduction of nickel. Apparently, Ni—Co alloy was not formed when Co and Ni were impregnated sequentially. Due to strong interaction of Co with the support material cobalt aluminate was first formed during the calcination step and then Ni was impregnated over this material. However, in the case of sequential impregnation of first Ni then Co (2.5Co@2.5Ni@SGA), a shallow and broad TPR peak was observed in the temperature range of 250–400 °C, in addition to the second sharp peak at around 750 °C. The shallow peak observed in the temperature range of 250–400 °C was associated to the partial reduction of cobalt oxide. The second sharp reduction peak observed at 750 °C was associated to the reduction of $NiAl_2O_3$. Apparently, in the case of successive impregnation of Ni and Co, nickel aluminate was formed during the calcination of this material at 800 °C. Cobalt was then impregnated on this material. Hence, formation of cobalt aluminate was significantly hindered in this case. Cobalt oxide deposited on $NiAl_2O_3$ was then reduced during the reduction process of the catalyst.

XRD patterns of mesoporous alumina (SGA), as well as the patterns of nickel, cobalt and nickel-cobalt incorporated SGA catalysts (5Ni@SGA, 5Co@SGA, 2.5Co-2.5Ni@SGA), which have been reduced at 750 °C, are shown in Fig. 7. XRD patterns of SGA showed typical peaks of γ-alumina at 2θ = 66.7° [440 plane], 46.2° [400 plane], 37.0° [311 plane], 39.5° [222 plane] etc. XRD patterns of 5Co@SGA clearly supported our conclusion that cobalt incorporated into this catalyst was not reduced to metallic Co^0. The main peak of Co^0 was expected at a 2θ value of about 44.23° (ICSD 15288) [30,37,45,47]. However, no such peak was observed at 2θ = 44.2°. Instead, a significant increase of the intensity of the peak at 36.6° was observed. The intensity ratio of the peaks observed at 36.6° and 46.2° was higher than 1.0 in the XRD patterns of 5Co@SGA. However this ratio was about 0.5 for pure SGA. The main XRD peak of cobalt aluminate ($CoAl_2O_4$) is expected at 2θ = 36.8° [48]. This result supported our conclusion that cobalt in the 5Co@SGA was most probably in the cobalt aluminate structure. Some contribution of Co_3O_4 to the XRD peak at 2θ = 36.6° is also a possibility, since the main XRD peak of this oxide is also expected at about 37° [311 plane] [30,45,47,49]. Both Co_3O_4 and $CoAl_2O_4$ have similar spinel structures and very similar XRD patterns [50]. However, these results proved that cobalt could not be reduced to metallic cobalt in the Co@SGA material, which was calcined at 800 °C. It is quite likely that cobalt oxide impregnated onto mesoporous alumina (SGA) strongly interacted with the support during the calcination step and converted to cobalt aluminate, which is extremely difficult to be reduced. Cobalt aluminate is also inactive in reforming reactions. Formation of $CoAl_2O_4$ was also reported in the literature at tem-

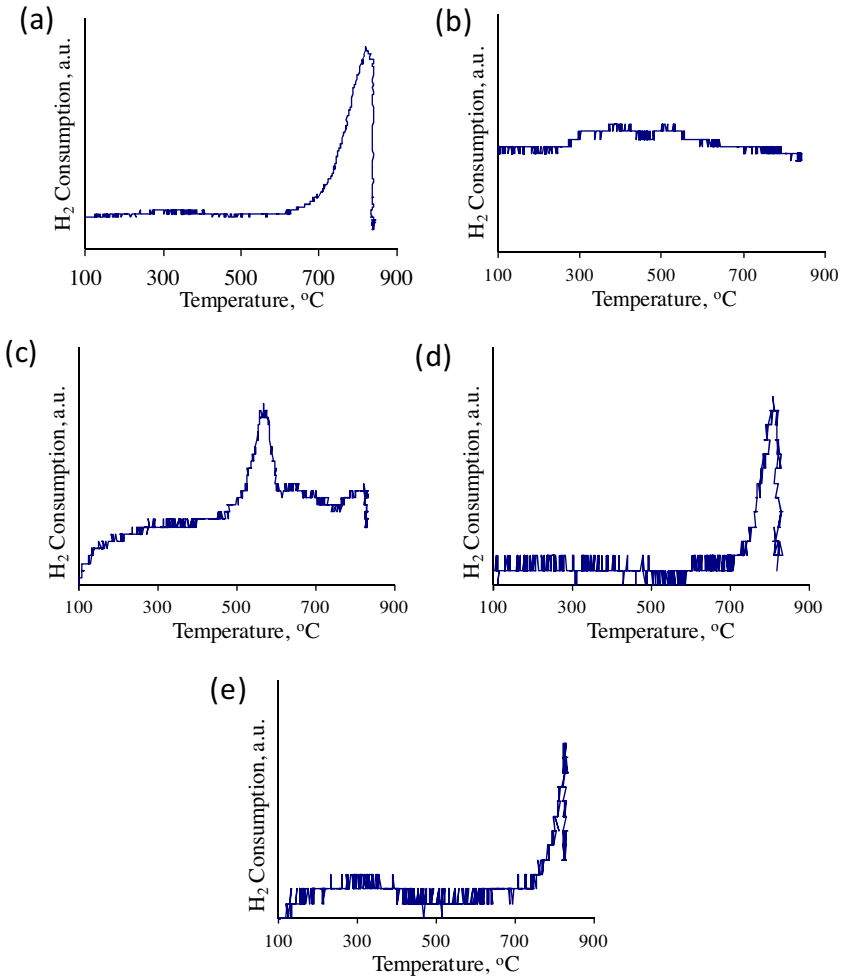

Fig. 6. TPR analysis of (a) calcined Ni@SGA, (b) calcined Co@SGA, (c) calcined 2.5Co-2.5Ni@SGA, (d) calcined 2.5Ni@2.5Co@SGA and (e) calcined 2.5Co@2.5Ni@SGA.

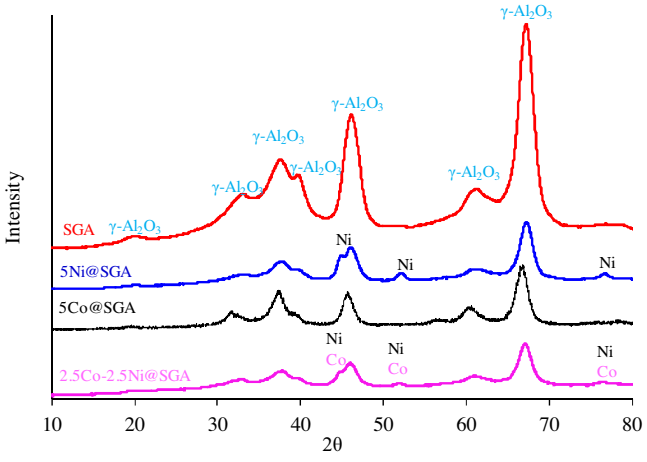

Fig. 7. XRD patterns of pure alumina (SGA), 5Ni@SGA, 5Co@SGA and bimetallic 2.5Co-2.5Ni@SGA catalysts, reduced at 750 °C.

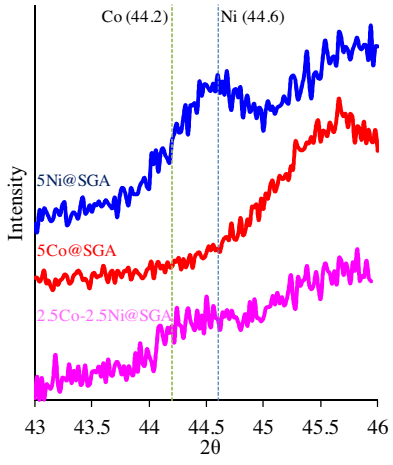

Fig. 8. XRD patterns of synthesized catalysts in the 2θ = 43–46° range.

peratures higher than 973 K, by UV–vis analysis of the synthesized materials [37,38].

In the XRD patterns of 5Ni@SGA, three additional peaks were observed at 44.6°, 51.8° and 76.9°, which were assigned to Ni. XRD patterns of the synthesized materials in the 43–46° region are shown in Fig. 8. In the case of 2.5Co-2.5Ni@SGA, the XRD peak at 44.6° was somewhat shifted to lower angles (to value of about 44.4°). Metallic cobalt was expected to give its strongest XRD peak at 44.2°, while the peak corresponding to Ni^0 was at 44.6°. Occurrence of a single peak at around 44.4° was assigned to the formation of a Ni—Co alloy. Similar conclusions were reported in the literature over different support materials [37,39]. XRD patterns of Co—Ni alloy nanoparticles synthesized by Ahmed et al. also supported this conclusion [51]. A small shift of the XRD peak of 5Ni@SGA at 51.9 to a lower angle of about 51.6 also supported the formation of Ni—Co

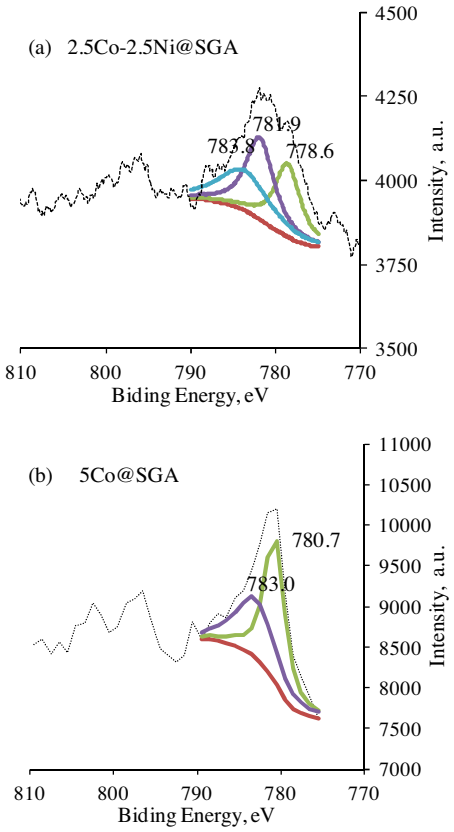

Fig. 9. XPS spectra (Co 2p region) of the catalysts reduced at 750 °C (a) 2.5Co-2.5Ni@SGA, (b) 5Co@SGA.

alloy (Fig. 7). As it was reported in the literature, reduction of Ni^{2+} was easier than reduction of Co^{2+}, and stabilization of cobalt was expected by the addition of nickel during the formation of Ni—Co alloy [52]. Formation of spinel type solid solution of Ni and Co oxides was also reported during calcination of bi-metallic MgO-ZrO_2 supported catalytic materials at 800 °C [29]. These results strongly supported our earlier TPR results, indicating cobalt and nickel in the bi-metallic 2.5Co-2.5Ni@SGA were easily reduced and this was the main reason of excellent catalytic performance of this material in dry reforming of methane.

In order to have a better understanding of the nature of Co compounds within the synthesized catalysts, their XPS analysis were also performed. XPS analysis results of cobalt compounds are available in number of publications in the literature [29,43,45–50,53,54]. A complete survey spectrum, as well as spectra for the regions for O 1s, C 1 s and Co 2p and Ni 2p, was collected for each catalyst sample. Collected data were corrected for charge shifting using standard C 1 s binding energy of 284.5 eV. XPS Peak 4.1 software package was used for curve fitting. Spectra were deconvoluted using Lorentzian–Gaussian combination peaks. X-ray photoelectron spectra of reduced catalysts 5Co@SGA and 2.5Co-2.5Ni@SGA, in the Co 2p region, are shown in Fig. 9. XPS analysis of 5Co@SGA showed Co 2p3/2 bands at 780.7 and 783.0 eV. Cobalt aluminate ($CoAl_2O_4$) was reported to have an electron binding energy of 780.6 eV [54]. Hence, XPS analysis result of 5Co@SGA strongly supported the formation of cobalt aluminate. Electron binding energies of CoO and Co_3O_4 were both reported as about 780 eV in the literature [50,54]. A peak at a higher binding energy (of about 784 eV) was generally associated to the synchronization of cobalt cations with hydroxil group due to chemical shift [29]. However, in the XPS spectrum of 2.5Co-2.5Ni@SGA, an additional peak was observed at 778.6 eV, with a tail extending to lower electron binding energies. This third peak observed at about 778.6 eV, proved the presence of Co^0 within this material. As it was discussed by Lebarbier et al. [47], Bayram et al. [45] and Mcintyre and Cook [54], an XPS peak at about 778–779 eV could be associated to Co^0. Although partial re-oxidation of reduced cobalt species is possible during the XPS analysis procedure, presence of the band at 778.6 eV in the XPS spectrum of 2.5Co-2.5Ni@SGA supported the conclusions reached from TPR and XRD analysis results that, Co^0 was present within this material. However, in the case of 5Co@SGA, there was no Co^0 species on the surface of this catalyst. Cobalt aluminate phase was formed in this case, due to strong interaction of cobalt and alumina during the heat treatment step. In the case of 2.5Co-2.5Ni@SGA, presence of Ni on the catalyst surface initiated formation of a Ni—Co alloy, which could be more easily reduced than 5Co@SGA and 5Ni@SGA. Quantitative analysis of the XPS data showed that at least 30% of cobalt compounds were in Co^0 state in the 2.5Co-2.5Ni@SGA.

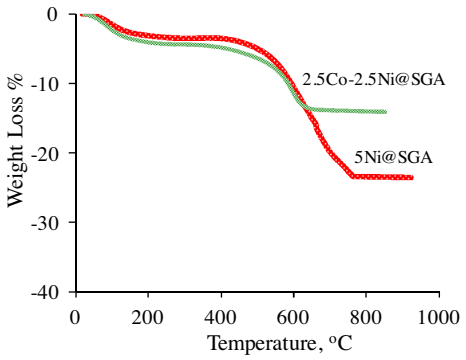

Fig. 10. TGA analysis of spent 5Ni@SGA and 2.5Co-2.5Ni@SGA catalysts after 4 h reaction tests.

3.3. Coke minimization as a result of Co incorporation

Coke formation on the surface of the catalysts during dry reforming tests was determined by thermal analysis (TGA-DTA) of the spent catalysts. These tests were performed in a flow of dry air, at a heating rate of 10 °C per minute. XRD analyses of the spent catalysts were also performed to observe crystalline form of coke, as well as morphological changes (if any) in the catalysts during dry reforming reaction tests. SEM image of the used catalyst was also obtained in order to observe the type of carbon formed on the catalyst surface.

The TGA analysis results of the used 5Ni@SGA and 2.5Co-2.5Ni@SGA catalysts, after 4 h activity tests performed at 600 °C, are shown in Fig. 10. Decrease of weight of the spent catalysts over 400 °C is mainly due to combustion of coke, which was deposited over the catalyst. As it was mentioned in the literature, oxidation of Ni to NiO may also cause some increase in the TGA curve in the temperature range of 230–500 °C [55]. However, maximum possible weight increase due to such re-oxidation of metals could be expected as about 1.2% and 0.6% for 5Ni@SGA and 2.5Co-2.5Ni@SGA, respectively.

As discussed in the previous sections, catalytic performance of the 2.5Co-2.5Ni@SGA catalyst was better than 5Ni@SGA catalyst, giving more stable selectivity values of H_2 and CO. Another positive effect of replacement of half of Ni in 5Ni@SGA catalyst with Co was found as the improvement achieved in coke minimization. As shown in the TGA of the spent catalysts (Fig. 10), amount of coke formed over 2.5Co-2.5Ni@SGA was less than half of the amount of coke formed over 5Ni@SGA at a reaction temperature of 600 °C. While the amount of coke formed over 5Ni@SGA was more than 20%, amount of coke formed over 2.5Co-2.5Ni@SGA was

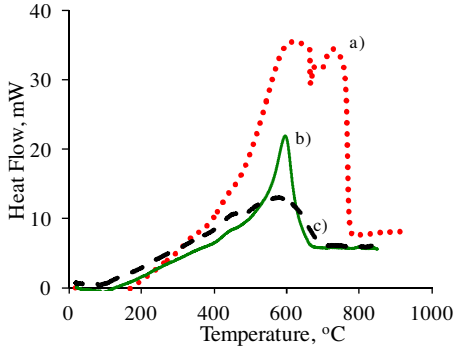

Fig. 11. Comparison of DTA profiles of spent catalysts after 4 h reaction tests; (a) 5Ni@SGA 600 °C, (b) 2.5Co-2.5Ni@SGA 600 °C, (c) 2.5Co-2.5Ni@SGA 750 °C..

about 10%, at the same reaction conditions. Coke minimization over 2.5Co-2.5Ni@SGA also helped to achieve more stable catalytic performance.

DTA analysis of the spent 2.5Co-2.5Ni@SGA (after 4 h reaction test) indicated only one broad oxidation peak of carbon in the temperature range of 200–650 °C (Fig. 11). This peak showed a maximum at a temperature of 590 °C. However, coke formed over 5Ni@SGA was oxidized giving two strong and broad exothermic DTA peaks at about 620 °C and 725 °C, indicating the presence of two different carbon species. Graphitic carbon was expected to be oxidized over 750 °C [10]. However, amorphous carbon was expected to be oxidized at temperatures lower than 500 °C [56]. Oxidation of filamentous carbon was also reported to take place in the temperature range of 500–650 °C [12]. These results indicated that coke formed over 2.5Co-2.5Ni@SGA was mainly in amorphous and filamentous form. SEM image of the spent 2.5Co-2.5Ni@SGA shown in Fig. 12 justified formation of some filamentous carbon at some locations over the surface of this catalyst. Diameters of these carbon filaments were estimated to be around 20 nm, from the SEM images.

XRD patterns of the spent catalysts were also consistent with the thermal analysis results. In the XRD patterns of the spent 2.5Co-2.5Ni@SGA, a very small carbon peak was observed at a 2θ value of about 26° (Fig. 13). However, for 5Ni@SGA, a highly strong carbon peak was observed, indicating the formation of crystalline carbon on the catalyst surface.

The main contributors to the formation of carbonaceous species on the catalyst surface were the dissociation of methane ($CH_4 \rightarrow C + 2H_2$) and Boudouard reaction ($2CO \rightarrow C + CO_2$). Methane decomposition is expected to gain importance at temperatures

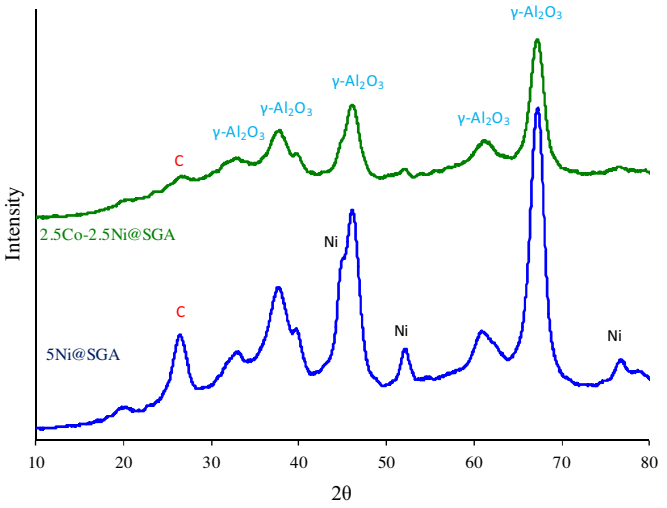

Fig. 13. XRD patterns of spent 5Ni@SGA and 2.5Co-2.5Ni@SGA catalysts after 4 h reaction tests.

higher than 600 °C [7,8,57] while the contribution of Boudouard reaction becomes more significant at lower temperatures. Origin and reactivity of carbon formed during dry reforming of methane over Ni impregnated ceria based catalysts was investigated in the recent work of Makri et al. [58]. Their work showed that, at 750 °C contributions of methane and CO_2 to the formation of inactive carbon were equally possible, while at 550 °C contribution of CO_2 was more significant. A mechanism consisting of dissociation of CO_2 to CO on the Ni sites and then conversion of adsorbed CO to carbon through a Boudouard reaction step was proposed to gain importance at lower temperatures. Dissociation of CO, which was produced through the dry reforming reaction was considered as an important source of inactive carbon formed on the catalyst surface, especially at lower temperatures. Although contribution of both coke formation mechanisms are quite probable at the reaction conditions of this work (600 °C), contribution of Boudouard reaction was expected to be more significant.

To see if there was any change in the pore structure of the synthesized materials after four hour reaction tests, nitrogen adsorption/desorption analyses of the spent catalysts were also obtained. Nitrogen adsorption/desorption isotherms of the fresh and spent 2.5Co-2.5Ni@SGA catalysts are shown in Fig. 14. As shown in this figure, the changes in the pore structure of this material after the reaction test was negligibly small. Both fresh and spent catalytic materials have mesoporous structures, showing Type IV

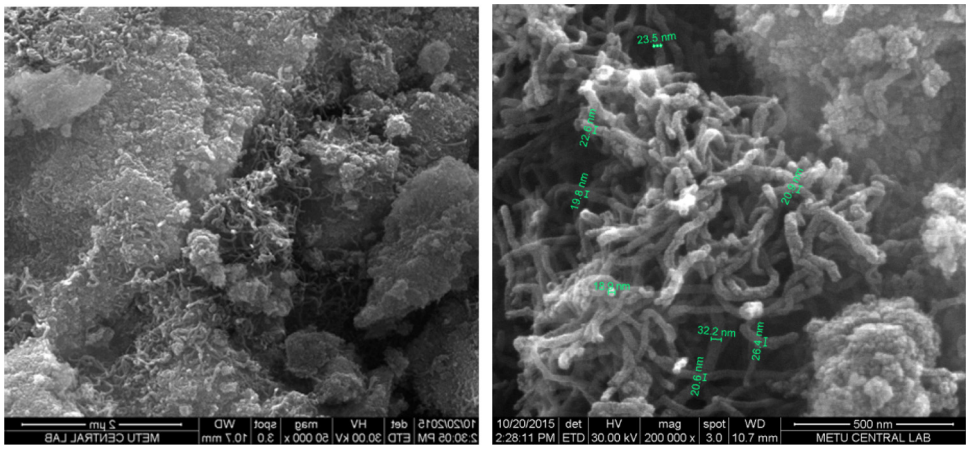

Fig. 12. SEM images of spent 2.5Co-2.5Ni@SGA catalyst.

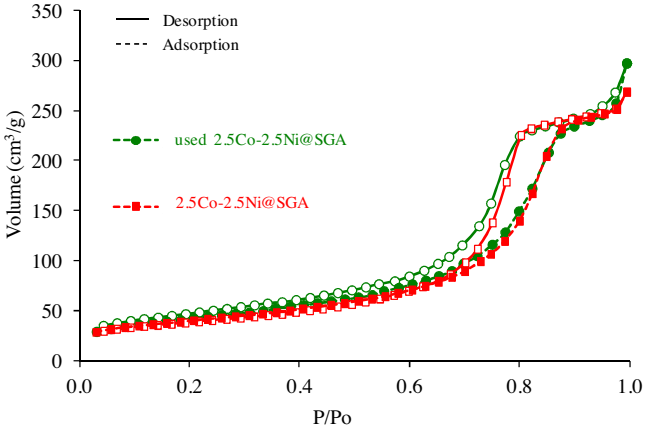

Fig. 14. N_2 adsorption/desorption isotherms of fresh and spent 2.5Co-2.5Ni@SGA.

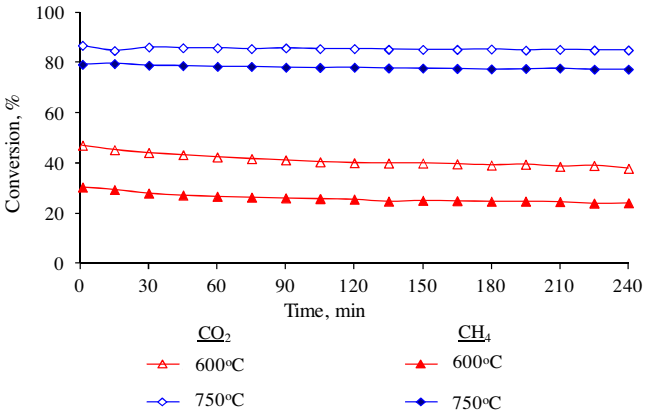

Fig. 15. Comparison of methane and carbon dioxide fractional conversion values obtained at 600 °C and 750 °C over 2.5Co-2.5Ni@SGA.

adsorption/desorption isotherms. Small changes observed in these isotherms are considered to be due to closure of some of the pores by deposited carbon during the reaction.

3.4. Effect of temperature on catalytic performance of 2.5Co-2.5Ni@SGA

As it was discussed in the previous sections, mesoporous alumina supported Co—Ni bimetallic catalyst (2.5Co-2.5Ni@SGA) showed much better catalytic performance in conversion of biogas to synthesis gas at 600 °C. To test the effect of temperature on the performance of this catalyst, dry reforming reaction was repeated at 750 °C. As shown in Fig. 15, increase of reaction temperature from 600 °C to 750 °C caused significant increase in the conversion values of both CH_4 and CO_2. In fact, conversion values of these two reactants approached to each other. Experimental conversion values of CH_4 and CO_2 (79% and 86%) were quite close to the equilibrium conversion values of 86% and 92%, respectively. Comparison of the performance of the 2.5Co-2.5Ni@SGA catalyst synthesized in the present study with the results reported in some of the recent publications on Ni and/or Co impregnated catalysts is given in Table 2. Besides the increase in conversion values, catalytic performance of 2.5Co-2.5Ni@SGA became more stable at 750 °C. Hydrogen and CO selectivity values observed during the reaction period of 4 h were highly stable (Fig. 16). Coke formed over this catalyst at 750 °C was about 8%. As shown in Fig. 11, DTA of spent catalyst after four hour reaction test at 750 °C gave a shallow exothermic peak in the temperature range of 250–650 °C. Thermodynamics of both RWGS

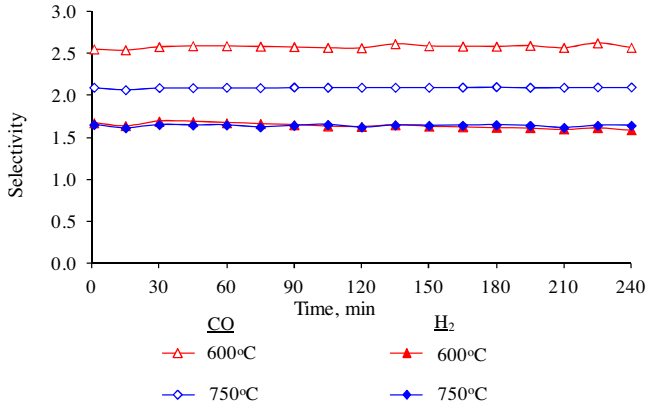

Fig. 16. Comparison of CO and H_2 selectivity values obtained at 600 °C and 750 °C over 2.5Co-2.5Ni@SGA.

reaction (R.2) and steam reforming of methane (R.4) are favored at 750 °C. Water formed as a result of RWGS reaction was expected to react with methane giving more hydrogen. Any coke formed as a result of methane decomposition would also react with CO_2 giving CO (reverse Boudouard reaction) at this reaction temperature.

4. Conclusions

Results of this work showed that mesoporous alumina supported Ni-Co impregnated bi-metallic material was a promising catalyst for dry reforming of methane. It was concluded that, replacement of half of Ni of nickel impregnated mesoporous alumina (5Ni@SGA) by cobalt (2.5Co-2.5Ni@SGA) significantly improved its catalytic performance, by increasing methane and carbon dioxide conversions, giving more stable hydrogen and CO selectivity values, as well as decreasing coke formation. Coke minimization achieved by Co incorporation helped to obtain more stable catalytic performance. Synthesis route and interaction of active metals with the support has important implications on the activity of mesoporous alumina supported catalysts. Cobalt should be in Co^0 state in order to show catalytic activity in dry reforming of methane. In the case of 2.5Co-2.5Ni@SGA, cobalt was shown to be in metallic state. However, in the catalyst containing only cobalt (i.e. 5Co@SGA), a Co—Al mixed oxide phase (cobalt aluminate) was formed during the calcination step of the catalyst at 800 °C. Since reducibility of cobalt aluminate was very low, this material showed no catalytic activity in dry reforming of methane. In the case of bimetallic catalyst prepared by simultaneous impregnation of Ni and Co (2.5Co-2.5Ni@SGA), an alloy of Ni—Co was formed, which was more easily reduced than both 5Co@SGA and 5Ni@SGA. Synergic effect of Ni and Co helped to improve the catalytic performance of Ni—Co impregnated mesoporous alumina. Increase of reaction temperature to 750 °C gave much more stable performance of 2.5Co-2.5Ni@SGA. In conclusion, it was shown that, mesoporous alumina supported bi-metallic Ni—Co was a highly promising catalyst for conversion of biogas to synthesis gas. In fact, the amount of coke formed over 2.5Co-2.5Ni@SGA was also low and mainly in amorphous form, which could be easily removed from the surface through air oxidation.

Acknowledgements

Scientific and Technological Research Council of Turkey (TUBITAK, Grant 111M449), collaboration between Gazi University, Middle East Technical University and Slovenian Institute of Chemistry, and Turkish Academy of Sciences (TÜBA) are gratefully acknowledged.

Table 2
Comparison of performances of Ni and/or Co based catalysts in dry reforming of CH_4.

Researcher	Catalyst	Reaction Condition	% CH_4 conversion
Aw et al. [2]	3.0%NiCo/CeZr c350	T: 750 °C P: 1.2 atm CH_4/CO_2: 1/1 WHSV: 12,000 ml/(gcat. h)	71
Osojnik et al. [4]	6NiCo-CeO_2-ZrO_2	T: 750 °C P: 1.2 atm CH_4/CO_2: 1/1 WHSV: 37,000 ml/(gcat. h)	37
Zhang et al. [28]	Ni—Co—Al—Mg—O	T: 750 °C P: 1 atm $CH_4/CO_2/N_2$: 1/1/1 WHSV: 110,000 ml/(gcat. h)	88
Fan et al. [29]	Ni—Co/MgO—ZrO_2	T: 750 °C P: 1 atm $CH_4/CO_2/N_2$: 1/1 WHSV: 125,000 ml/(gcat. h)	80
Arbag et al. [12]	5Ni-SGA	T: 750 °C P: 1 atm $CH_4/CO_2/Ar$ = 1/1/1 WHSV: 36,000 ml/(gcat. h)	70
This work	2.5Co-2.5Ni@SGA	T: 750 °C P: 1 atm $CH_4/CO_2/Ar$ = 1/1/1 WHSV: 36,000 ml/(gcat. h)	79
Wu and Chou [15]	Rh1Ni1/Boron nitride	T: 700 °C P: 1 atm CH_4/CO_2: 1/1 WHSV: 60,000 ml/(gcat. h)	42
San-Joseí-Alonso et al. [17]	Ni(9)-γ-alumina	T: 700 °C P: 1 atm CH_4/CO_2: 1/1 WHSV: 20,000 ml/(gcat. h)	60
Wang et al. [19]	Ni/Ce-SBA-15	T: 700 °C P: 1 atm CH_4/CO_2: 1/1 WHSV: 36,000 ml/(gcat. h)	77
Luisetto et al. [22]	Co—Ni/CeO_2	T: 600 °C P: 1 atm CH_4/CO_2/Ar: 1/1/3 WHSV: 30,000 ml/(gcat. h)	48
Yu et al. [24]	NiMgAlLa	T: 600 °C P: 1 atm CH_4/CO_2: 1/1 WHSV: 7200 h^{-1}	45
Arbag et al. [27]	Ni-MCM-41	T: 600 °C P: 1 atm $CH_4/CO_2/Ar$ = 1/1/1 WHSV: 36,000 ml/(gcat. h)	28
This work	2.5Co-2.5Ni@SGA	T: 600 °C P: 1 atm $CH_4/CO_2/Ar$ = 1/1/1 WHSV: 36,000 ml/(gcat. h)	30

References

[1] X. Verykios, Int. J. Hydrogen Energy 28 (2003) 1045–1063.
[2] M.S. Aw, I.G.Č. Osojnik, A. Pintar, Catal. Sci. Technol. 4 (2014) 1340–1349.
[3] U. Izquierdo, V.L. Barrio, K. Bizkarra, A.M. Gutierrez, J.R. Arrabi, L. Gartzia, J. Banuelos, I. Lopez-Arbeloa, J.F. Cambra, Chem. Eng. J. 238 (2014) 178–188.
[4] I.G.Č. Osojnik, P. Djinović, B. Erjavec, A. Pintar, Chem. Eng. J. 207 (2012) 299–307.
[5] H. Arbag, S. Yasyerli, N. Yasyerli, T. Dogu, G. Dogu, Top. Catal. 56 (2013) 1695–1707.
[6] A.F. Cunha, J.J.M. Orfao, J.L. Figueiredo, Appl. Catal. A: Gen. 348 (2008) 103–112.
[7] A.F. Cunha, J.J.M. Orfao, J.L. Figueiredo, Int. J. Hydrogen Energy 34 (2009) 4763–4772.
[8] P. Djinović, I.G.Č. Osojnik, B. Erjavec, A. Pintar, Appl. Catal. B: Environ. 125 (2012) 259–270.
[9] N. Laosinpojana, W. Sutthisripok, S. Assabumrungrat, Chem. Eng. J. 112 (2005) 13–22.
[10] H. Mustu, S. Yasyerli, N. Yasyerli, G. Dogu, T. Dogu, P. Djinovic, A. Pintar, Int. J. Hydrogen Energy 40 (2015) 3217–3228.
[11] K. Nagaoka, M. Okamura, K. Aika, Catal. Commun. 2 (2001) 255–260.
[12] H. Arbag, S. Yasyerli, N. Yasyerli, G. Dogu, T. Dogu, I.G.Č. Osojnic, A. Pintar, Ind. Eng. Chem. Res. 54 (2015) 2290–2301.
[13] V.R. Choudary, K.C. Mondal, T.V. Choudary, Chem. Eng. J. 121 (2006) 73–77.
[14] S. Ozkara-Aydinoglu, A.E. Aksoylu, Chem. Eng. J. 215 (2012) 542–549.
[15] J.C.S. Wu, H.C. Chou, Chem. Eng. J. 148 (2009) 539–545.
[16] S. Ozkara-Aydinoglu, E. Ozensoy, E.A. Aksoylu, Int. J. Hydrogen Energy 34 (2009) 9711–9722.
[17] D. San-Jose-Alonso, J. Juan-Juan, M.J. Illan-Gomez, M.C. Roman-Martinez, Appl. Catal. A: Gen. 371 (2009) 54–59.

[18] Z. Hou, P. Chen, H. Fang, X. Zheng, T. Yashima, Int. J. Hydrogen Energy 31 (2006) 555–561.
[19] N. Wang, W. Chu, T. Zhang, Z.S. Zhao, Int. J. Hydrogen Energy 37 (2012) 19–30.
[20] S. Ozkara-Aydinoglu, E. Aksoylu, Catal. Commun. 11 (2010) 1165–1170.
[21] Z. Alipour, M. Rezaei, F. Meshkani, Fuel 129 (2014) 197–203.
[22] I. Luisetto, S. Tuti, E.D. Bartolomeo, Int. J. Hydrogen Energy 37 (2012) 15992–15999.
[23] C. Cheng, W. Huang, Fuel Process. Technol. 91 (2010) 185–193.
[24] X.P. Yu, N. Wang, W. Chu, M. Liu, Chem. Eng. J. 209 (2012) 623–632.
[25] S. Yasyerli, S. Filizgok, H. Arbag, N. Yasyerli, G. Dogu, Int. J. Hydrogen Energy 36 (2011) 4863–4874.
[26] M.M. Barroso-Quiroga, A.E. Castro-Luna, Int. J. Hydrogen Energy 35 (2010) 6052–6056.
[27] H. Arbag, S. Yasyerli, N. Yasyerli, G. Dogu, Int. J. Hydrogen Energy 35 (2010) 2296–2304.
[28] J. Zhang, H. Wang, A.K. Dalai, J. Catal. 249 (2007) 300–310.
[29] M.S. Fan, A.Z. Abdullah, S. Bhatia, Appl. Catal. B: Environ. 100 (2010) 365–377.
[30] S. Gunduz, T. Dogu, Appl. Catal. B: Environ. 168 (2015) 497–508.
[31] K. Tao, L. Shi, Q. Ma, D. Wang, C. Zeng, C. Kong, M. Wu, L. Chen, S. Zhou, Y. Hu, N. Tsubaki, Chem. Eng. J. 221 (2013) 25–31.
[32] N. Wang, X. Yu, Y. Wang, W. Chu, M. Liu, Catal. Today 212 (2013) 98–107.
[33] W. Nimwattanakul, A. Luengnaruemitchai, S. Jitkarnka, Int. J. Hydrogen Energy 31 (2006) 93–100.
[34] K. Takanabe, K. Nagaoka, K. Nariai, K. Aika, J. Catal. 230 (2005) 75–85.
[35] O. Gonzalez, J. Lujano, E. Pietri, M.R. Goldwasser, Catal. Today 107–108 (2005) 436–443.
[36] S. Damyanova, B. Pawalec, K. Arishtirova, J.L.G. Fierro, C. Sener, T. Dogu, Appl. Catal. B: Environ. 92 (2009) 250–261.
[37] K. Takanabe, K. Nagaoka, K. Nariai, K. Aika, J. Catal. 232 (2005) 268–275.
[38] T. Das, G. Deo, J. Mol. Catal. A: Chem. 350 (2011) 75–82.
[39] S. Sengupta, K. Ray, G. Deo, Int. J. Hydrogen Energy 39 (2014) 11462–11472.
[40] P. Kim, Y. Kim, H. Kim, I.K. Song, J. Yi, Appl. Catal. A: Gen. 272 (2004) 157–166.
[41] Y.J.O. Asencios, K.F.M. Elias, E.M. Assaf, Appl. Surf. Sci. 317 (2014) 350–359.
[42] O. Joo, K. Jung, Bull. Korean Chem Soc. 23 (2002) 1149–1153.
[43] W. Chu, P.A. Chernavskii, L. Gengembre, G.A. Pankina, P. Fongarland, A.Y. Khodakov, J. Catal. 252 (2007) 215–230.
[44] K. Shimura, T. Miyazawa, T. Hanaoka, S. Hirata, J. Mol. Catal. A: Chem. 407 (2015) 15–24.
[45] B. Bayram, I.I. Soykal, D. Von Deak, J.T. Miller, U.S. Ozkan, J. Catal. 284 (2011) 77–89.
[46] A.M. Karim, Y. Su, M.H. Engelhard, D.I. King, Y. Wang, ACS Catal. 1 (2011) 279–286.
[47] B.M. Lebarbier, A.M. Karim, M.H. Engelhard, Y. Wu, B.Q. Xu, E.J. Petersen, A. Datye, Y. Wang, ChemSusChem 4 (2011) 1679–1684.
[48] S. Ummartyotin, S. Sangngerns, A. Kaewvilai, N. Koonsaeng, H. Manuspiya, A. Laobothee, J. Sustainable Energy Environ. 1 (2009) 31–37.
[49] W. Yue, W. Zhou, J. Mater. Chem. 17 (2007) 4947–4952.
[50] Zs. Ferencz, K. Baan, A. Oszko, Z. Konya, T. Kecskes, A. Erdöhelyi, Catal. Today 228 (2014) 123–130.
[51] J. Ahmed, S. Sharma, K.V. Ramanujachary, S.E. Lofland, A.K. Ganguli, J. Coll. Interface Sci. 336 (2009) 814–819.
[52] Y.D. Li, L.Q. Li, H.W. Liao, H.R. Wang, J. Mater. Chem. 9 (1999) 2675–2677.
[53] N. Srisawad, W. Chaitree, O. Mekasuwandumrong, P. Praserthdam, J. Panpranot, J. Nanomater. 2012 (2012) (Article ID 108369).
[54] M.S. Mcintyre, M.G. Cook, Anal. Chem. 47 (1975) 2208–2213.
[55] A.D.D. Kaynar, D. Dogu, N. Yasyerli, Fuel Proc. Technol. 140 (2015) 96–103.
[56] D. Liu, X.Y. Quek, W.N.E. Cheo, R. Lau, A. Borgna, Y. Yang, J. Catal. 266 (2009) 380–390.
[57] M.A. Ermakova, D.Y. Ermakov, A.L. Chuvilin, G.G. Kuvshinov, J. Catal. 201 (2001) 183–197.
[58] M.M. Makri, M.A. Vasiliades, K.C. Petallidou, A.M. Efstathiou, Catal. Today 259 (2015) 150–164.